Medicinal Chemistry Research
https://doi.org/10.1007/s00044-020-02634-0

MEDICINAL CHEMISTRY RESEARCH

ORIGINAL RESEARCH

Novel amide analogues of quinazoline carboxylate display selective antiproliferative activity and potent EGFR inhibition

Anjleena Malhotra[1] · Ranju Bansal[1] · Clarissa Esmeralda Halim[2] · Celestial T. Yap[2] · Gautam Sethi[3] · Alan Prem Kumar[3,4,5] · Mahendra Bishnoi[6] · Kamalendra Yadav[6]

Received: 7 March 2020 / Accepted: 8 September 2020

Abstract

In the present study, a novel series of quinazoline derivatives is developed for cancer therapy. All the synthesised analogues were evaluated against a panel of 60 human cancer cell lines for the antiproliferative activity. Significant and selective growth inhibition of several solid tumour cell lines such as NCI-H322M, NCI-H522 (non-small cell lung cancer), IGROV1, SK-OV-3 (ovarian cancer), TK-10 (renal cancer) and MDA-MB-468 (breast cancer) was observed. Further, all the new amide analogues strongly inhibited EGFR in low nanomolar range with morpholino quinazoline **10** producing activity ($IC_{50} = 6.12$ nM) comparable to standard drugs erlotinib and gefitinib. In addition, western blot analysis depicted inhibition of phosphorylation of EGFR by compounds **10** and **11** in MDA-MB-468 cells at 10 μM. Molecular docking studies showed the strong binding interactions with the active site of the EGFR protein. The current investigation could be extremely helpful for the development of newer therapeutically useful quinazoline based molecules for cancer therapy.

Keywords Quinazoline · EGFR inhibitors · Antiproliferative activity

Introduction

The epidermal growth factor receptor (EGFR) belongs to receptor tyrosine kinase group, which regulates several functions of cellular proliferation, adhesion, migration, survival and differentiation through various signal transduction pathways [1, 2]. Overexpression of EGFR results not only in progression of wide variety of solid tumours including non-small cell lung, breast, colorectal, renal, head, neck, bladder, ovarian cancers but also decreases sensitivity of cells to conventional chemotherapeutic agents [3, 4]. Inhibition of EGFR has emerged as an eye-catching target for anticancer therapy over the years [5, 6]. Though over the past decade, many advances in EGFR related carcinoma therapeutics have taken place, there is still ample scope for improvement. Development of resistance and several side effects associated with the available drugs acting through this mechanism give rise to an exigent necessity to develop therapeutically useful potent small molecule EGFR inhibitors for cancer therapy [7, 8].

Gefitinib (Iressa®) is the first-generation reversible EGFR inhibitor, which has been approved by US Food and Drug Administration (FDA) for the first line treatment of non-small cell lung cancer [9, 10]. However, limited usage of reversible EGFR inhibitors due to emergence of resistance resulted in development of second-generation irreversible inhibitors, e.g. afatinib (Gilotrif®), which binds with the tyrosine kinase enzyme through a covalent bond [11]. Due to irreversible binding, ATP are not able to displace these inhibitors, which leads to prevalence of nonspecific reactions with other targeted biomolecules resulting in several

Supplementary information The online version of this article (https://doi.org/10.1007/s00044-020-02634-0) contains supplementary material, which is available to authorized users.

✉ Ranju Bansal
ranju29in@yahoo.co.in

1 University Institute of Pharmaceutical Sciences, Panjab University, Chandigarh, India

2 Department of Physiology, Yong Loo Lin School of Medicine, National University of Singapore, Singapore, Singapore

3 Department of Pharmacology, Yong Loo Lin School of Medicine, National University of Singapore, Singapore, Singapore

4 Medical Science Cluster, Yong Loo Lin School of Medicine, National University of Singapore, Singapore, Singapore

5 Cancer Science Institute of Singapore, National University of Singapore, Singapore, Singapore

6 National Agri-Food Biotechnology Institute, Mohali, Punjab, India

Published online: 19 September 2020

serious toxic effects of second-generation inhibitors [12, 13]. Therefore, it is highly desired to discover safer, potent and reversible inhibitors of EGFR.

Chemically, both gefitinib and afatinib are 4-anilinoquinazoline analogues. 4-Anilinoquinazoline derivatives serve as lead compounds for EGFR kinase inhibition. Literature indicates that the important structural parameters required for tyrosine kinase inhibitory activity include (i) free -NH linker at 4-position of quinazoline (ii) hydrogen bonding interaction of N^1 of quinazoline moiety (iii) electron-donating group at the 6- and/or 7-positions of quinazolines and (iv) small substituents preferentially halogens on the aniline moiety [14–16]. In order to reduce the incidence of developing mutation related resistance against gefitinib like molecules, the morpholinopropoxy group at 6- position of quinazoline ring has been replaced by a Michael acceptor functionality in the new generation EGFR inhibitors such as afatinib [17]. The α,β-unsaturated carbonyl moiety of these second-generation inhibitors forms a Michael adduct through covalent bonding with Cys797 amino acid of EGFR. But serious side effects associated with these irreversible inhibitors limits their usefulness.

Keeping these observations in mind, it was planned to design and synthesise some new gefitinib based quinazoline derivatives by incorporating structural features of both 1st generation and 2nd generation inhibitors to obtain potent EGFR inhibitory analogues having enhanced selectivity against solid tumour cell lines overexpressing EGFR (Fig. 1). The lead molecule gefitinib possesses three carbon atoms in the side chain at 6- position of quinazoline ring while afatinib is substituted with four carbon atom moiety. In the proposed molecules, a two carbon spacer has been introduced between quinazoline nucleus and the terminal nitrogen to study the SAR of quinazoline based anticancer agents. The synthesised analogues have been examined for their antiproliferative effects on cancer cell lines and inhibitory activity against EGFR tyrosine kinase. In addition, western blot analysis to gain mechanistic insights and molecular docking to study the receptor-ligand interactions were also performed.

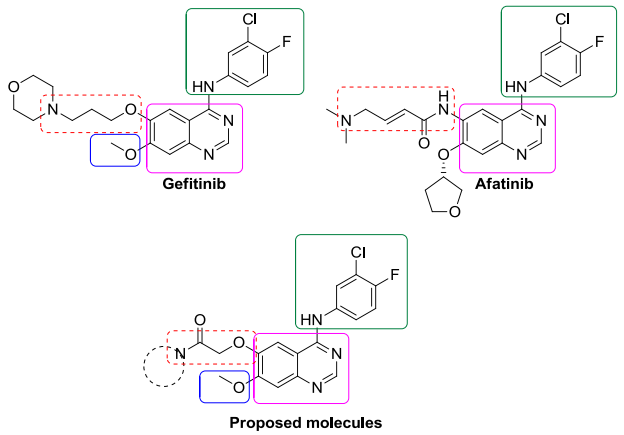

Fig. 1 Structures of clinically available quinazolines gefitinib and afatinib and proposed molecules

Materials and methods

Chemistry

The melting points (uncorrected) were taken on Veego melting point apparatus (Veego, Mumbai, India). IR spectra were recorded using KBr pellet method on Spectrum Two model spectrophotometer (Perkin Elmer, USA). Bruker Avance II spectrophotometer (Bruker AG, Switzerland) was used to study ^{1}H NMR (400 MHz) and ^{13}C NMR (100 MHz) spectra. Deuterated chloroform ($CDCl_3$) or deuterated dimethyl sulfoxide (DMSO-d_6) were used as solvents for NMR studies with tetramethyl silane (TMS) as internal standard (chemical shifts were recorded in δ ppm). The spin multiplicities are mentioned as symbols s (singlet), d (doublet), t (triplet), q (quartet), dd (doublet of doublet), m (multiplet) and br (broad). Mass spectra were determined using electrospray ionisation technique on Waters Micromass Q-Tof spectrometer and Agilent 1100 LC coupled with Bruker made mass spectrometer model Esquire 3000. Elemental analysis was carried out on Thermo Scientific (Flash 2000) CHN elemental analyser. A slurry of silica gel G in ethyl acetate was used for preparing thin layer chromatography (TLC) plates as per Stahl method. The plates were activated at 110 °C for 30 min and iodine chamber was used for visualising the spots. All the solvents used for the synthesis of the compounds were distilled prior to use as per standard procedure. Anhydrous sodium sulphate was used as drying agent. In vitro cancer cell line assay of all the synthesised compounds was carried out at NCI, USA.

Synthesis of methyl 2-(4-(3-chloro-4-fluorophenylamino)-7-methoxyquinazolin-6-yloxy) acetate (9)

Methyl chloroacetate (0.1 mL, 0.94 mmol) was added to a stirred and heated suspension of 4-(3-chloro-4-fluorophenylamino)-7-methoxyquinazolin-6-ol (**8**, 0.15 g, 0.47 mmol) and K_2CO_3 (0.15 g) in DMF (3 mL). The reaction mixture was further heated at 80 °C for 5 h with continuous stirring, the reaction being monitored by TLC. On completion, reaction mixture was filtered and cold water was added to the filtrate. The precipitated material was filtered and recrystallised from methanol to obtain **9**. Yield (0.093 g, 50.54%), m.p. 224–226 °C. FT-IR ν_{max} (KBr): 3411.03 (N–H), 2954.29 (asymmetric aliphatic C–H), 2847.00 (symmetric aliphatic C–H), 1735.38 (ester C=O),

1627.29, 1580.94 (C=N), 1503.94, 1433.90, 1285.87, 1213.05 (asymmetric C–O–C), 1121.02 (C–F), 1073.03 (C–Cl), 1039.80 (symmetric C–O–C), 852.71 cm^{-1}. ^{1}H NMR (DMSO-d_6): δ 3.81 (s, 3H, -COOCH_3), 4.00 (s, 3H, -OCH_3), 4.93 (s, 2H, -OCH_2-), 7.21 (s, 1H, Ar*H*, quinazoline), 7.25 (t, 1H, $J_o = 8.92$ Hz, Ar*H, ortho* to fluoro), 7.74–7.78 (m, 1H, Ar*H*, *ortho* to chloro), 7.82 (s, 1H, Ar*H*, quinazoline), 8.03 (dd, 1H, $J_o = 6.76$ Hz, $J_m = 2.60$ Hz, Ar*H*, *meta* to fluoro), 8.50 (s, 1H, -N=C*H*-N) and 9.37 ppm (s, 1H, -N*H*-). ^{13}C NMR (DMSO-d_6): δ 51.73 (COO**C**H_3), 55.67 (O**C**H_3), 65.37 (O**C**H_2), 103.45 (Ar**C**H), 107.35 (Ar**C**H), 108.62 (Ar**C**), 115.88 (Ar**C**H, $^2J_{C\text{-}F} = 21$ Hz), 119.21 (Ar**C**, $^2J_{C(Cl)\text{-}F} = 18$ Hz), 121.92 (Ar**C**H, $^3J_{C\text{-}F} = 6$ Hz), 123.63 (Ar**C**H), 136.19 (Ar**C**, $^4J_{C\text{-}F} = 4$ Hz), 147.31 (Ar**C**), 147.83 (Ar**C**), 152.88 (N=**C**H-N), 153.40 (Ar**C**, $^1J_{C\text{-}F} = 242$ Hz), 154.15 (Ar**C**), 156.15 (Ar**C**) and 168.18 ppm (**C**=O). Anal. calcd for $C_{18}H_{15}ClFN_3O_4$: C, 55.18; H, 3.86; N, 10.73%. Found: C, 54.95; H, 4.06; N, 10.94%.

General procedure for the synthesis of amide analogues 10–17

A mixture of ester **9** (0.2 g, 0.51 mmol) and required amine (0.5 mL, in excess) was fused (3–6 h) at 90 °C with continuous stirring. The reaction was monitored by TLC. Ice cold water was added to the reaction mixture on completion of the reaction. The precipitate obtained was filtered, washed several times with distilled water and dried. Crystallised from methanol gave the corresponding desired analogue **10–17**.

4-(3-Chloro-4-fluorophenylamino)-7-methoxy-6-[2-(morpholin-4-yl)-2-oxo]ethoxyquinazoline (**10**) Yield (0.11 g, 48.25%), m.p. 224–226 °C. FT-IR ν_{max} (KBr): 3360.52 (N–H), 2980.41 (asymmetric aliphatic C–H), 2861.21 (symmetric aliphatic C–H), 1648.82 (amide C=O), 1628.50, 1582.31 (C=N), 1504.22, 1431.72, 1273.64, 1234.05 (asymmetric C–O–C), 1121.02 (C–F), 1064.69 (C–Cl), 1030.40 (symmetric C-O-C), 851.13 cm^{-1}. ^{1}H NMR (DMSO-d_6): δ 3.56 (br s, 4H, -N(CH_2)$_2$-, morpholine), 3.63 (br s, 2H, -OCH_2-, morpholine), 3.69 (br s, 2H, -OCH_2-, morpholine), 3.97 (s, 3H, -OCH_3), 4.96 (s, 2H, -OCH_2-), 7.21 (s, 1H, Ar*H*, quinazoline), 7.36 (t, 1H, $J_o =$ 9.02 Hz, Ar*H, ortho* to fluoro), 7.76–7.79 (m, 1H, Ar*H*, *ortho* to chloro), 7.80 (s, 1H, Ar*H*, quinazoline), 8.13 (dd, 1H, $J_o = 6.82$ Hz, $J_m = 2.58$ Hz, Ar*H*, *meta* to fluoro), 8.50 (s, 1H, -N = C*H*-N) and 9.45 ppm (s, 1H, -N*H*-). ^{13}C NMR (DMSO-d_6): δ 41.78 (N**C**H_2, morpholine), 45.26 (N**C**H_2, morpholine), 55.81 (O**C**H_3), 66.10 (2 × O**C**H_2, morpholine), 67.22 (O**C**H_2), 103.67 (Ar**C**H), 107.36 (Ar**C**H), 108.61 (Ar**C**), 116.27 (Ar**C**H, $^2J_{C\text{-}F} = 21$ Hz), 118.94 (Ar**C**, $^2J_{C(Cl)\text{-}F} = 18$ Hz), 121.90 (Ar**C**H, $^3J_{C\text{-}F} = 7$ Hz), 123.23 (Ar**C**H), 136.59 (Ar**C**, $^4J_{C\text{-}F} = 3$ Hz), 147.22 (Ar**C**), 147.29 (Ar**C**), 152.78 (N = **C**H-N), 153.20 (Ar**C**, $^1J_{C\text{-}F} = 249$ Hz), 154.37 (Ar**C**), 156.03 (Ar**C**) and 165.24 ppm (**C**=O). ESI-MS m/z: 447.35 $[M + H]^+$, 449.36 $[MH + 2]^+$, 469.37 $[M + Na]^+$. Anal. calcd for $C_{21}H_{20}ClFN_4O_4$: C, 56.44; H, 4.51; N, 12.54%. Found: C, 56.04; H, 4.82; N, 12.90%.

4-(3-Chloro-4-fluorophenylamino)-7-methoxy-6-[2-(piperidin-1-yl)-2-oxo]ethoxyquinazoline (**11**) Yield (0.12 g, 52.86%), m.p. 218–220 °C. FT-IR ν_{max} (KBr): 3337.61 (N–H), 2938.22 (asymmetric aliphatic C–H), 2860.24 (symmetric aliphatic C–H), 1631.38 (amide C=O), 1575.81 (C=N), 1504.13, 1428.51, 1232.73 (asymmetric C–O–C), 1136.06 (C–F), 1064.95 (C–Cl), 1008.09 (symmetric C–O–C), 845.93 cm^{-1}. ^{1}H NMR ($CDCl_3$): δ 1.49 (br s, 2H, -CH_2-, piperidine), 1.64 (br s, 4H, 2 × -CH_2-, piperidine), 3.53 (br s, 4H, -N(CH_2)$_2$-, piperidine), 3.86 (s, 3H, -OCH_3), 4.95 (s, 2H, -OCH_2-), 7.00 (s, 1H, Ar*H*, quinazoline), 7.04 (t, 1H, $J_o = 8.82$ Hz, Ar*H*, *ortho* to fluoro), 7.51–7.55 (m, 1H, Ar*H*, *ortho* to chloro), 7.65 (s, 1H, Ar*H*, quinazoline), 7.70 (dd, 1H, $J_o = 6.64$ Hz, $J_m = 2.60$ Hz, Ar*H*, *meta* to fluoro), 8.54 (s, 1H, -N = C*H*-N) and 8.56 ppm (br s, 1H, -N*H*). ^{13}C NMR ($CDCl_3$): δ 24.25 (**C**H_2, piperidine), 25.52 (**C**H_2, piperidine) 26.34 (**C**H_2, piperidine), 43.47 (N**C**H_2, piperidine), 46.58 (N**C**H_2, piperidine), 55.98 (O**C**H_3), 67.92 (O**C**H_2), 104.07 (Ar**C**H), 107.55 (Ar**C**H), 108.88 (Ar**C**), 116.10 (Ar**C**H, $^2J_{C\text{-}F} =$ 22 Hz), 120.29 (Ar**C**, $^2J_{C(Cl)\text{-}F} = 18$ Hz), 121.78 (Ar**C**H, $^3J_{C\text{-}F} = 6$ Hz), 123.85 (Ar**C**H), 135.68 (Ar**C**), 147.05 (Ar**C**), 147.46 (Ar**C**), 153.58 (N = **C**H-N), 154.35 (Ar**C**, $^1J_{C\text{-}F} =$ 244 Hz), 154.59 (Ar**C**), 156.51 (Ar**C**) and 166.55 ppm (**C**=O). ESI-MS m/z: 445.38 $[M + H]^+$, 447.38 $[MH + 2]^+$, 467.38 $[M + Na]^+$. Anal. calcd for $C_{22}H_{22}ClFN_4O_3$: C, 59.39; H, 4.98; N, 12.59%. Found: C, 59.24; H, 4.72; N, 12.88%.

4-(3-Chloro-4-fluorophenylamino)-7-methoxy-6-[2-(N-methylpiperazin-1-yl)-2-oxo]ethoxy-quinazoline (**12**) Yield (0.132 g, 56.41%), m.p. 231–232 °C. FT-IR ν_{max} (KBr): 3351.35 (N–H), 3074.25 (aromatic C–H), 2940.01 (asymmetric aliphatic C–H), 2851.06 (symmetric aliphatic C–H), 1642.86 (amide C=O), 1581.16 (C=N), 1505.56, 1433.54, 1296.45, 1243.03 (asymmetric C–O–C), 1144.39 (C–F), 1078.49 (C-Cl), 1049.30 (symmetric C–O–C), 847.71 cm^{-1}. ^{1}H NMR (DMSO-d_6): δ 2.29 (s, 3H, -NCH_3, piperazine), 2.39 (br s, 2H, -NCH_2-, piperazine), 2.47 (br s, 2H, -NCH_2-, piperazine), 3.62 (t, 4H, $J = 4.84$ Hz, -N(CH_2)$_2$-, piperazine), 3.99 (s, 3H, -OCH_3), 4.94 (s, 2H, -OCH_2-), 7.19 (s, 1H, Ar*H*, quinazoline), 7.21 (t, 1H, $J_o = 8.88$ Hz, Ar*H*, *ortho* to fluoro), 7.75–7.79 (m, 1H, Ar*H*, *ortho* to chloro), 7.82 (s, 1H, Ar*H*, quinazoline), 8.06 (dd, 1H, $J_o = 6.72$ Hz, $J_m = 2.52$ Hz, Ar*H*, *meta* to fluoro), 8.51 (s, 1H, -N = C*H*-N) and 9.41 ppm (s, 1H, -N*H*-). ^{13}C NMR (DMSO-d_6): δ 41.33 (N**C**H_3, piperazine), 44.55 (N**C**H_2, piperazine), 45.51, (N**C**H_2, piperazine), 54.07 (N**C**H_2, piperazine), 54.53 (N**C**H_2, piperazine) 55.61 (O**C**H_3), 67.38 (O**C**H_2), 103.58 (Ar**C**H), 107.36 (Ar**C**H), 108.70 (Ar**C**), 115.80

(Ar**C**H, $^2J_{C\text{-}F} = 22$ Hz), 119.29 (Ar**C**, $^2J_{C(Cl)\text{-}F} = 18$ Hz), 121.67 (Ar**C**H, $^3J_{C\text{-}F} = 6$ Hz), 123.41 (Ar**C**H), 136.18 (Ar**C**, $^4J_{C\text{-}F} = 3$ Hz), 147.01 (Ar**C**), 147.16 (Ar**C**), 152.78 (Ar**C**), 153.38 (Ar**C**, $^1J_{C\text{-}F} = 243$ Hz), 154.32 (N = **C**H-N), 156.16 (Ar**C**) and 165.10 ppm (**C**=O). ESI-MS m/z: 460.40 $[M + H]^+$, 462.41 $[MH + 2]^+$, 482.41 $[M + Na]^+$. Anal. calcd for $C_{22}H_{23}ClFN_5O_3$: C, 57.46; H, 5.04; N, 15.23%. Found: C, 57.74; H, 5.22; N, 15.41%.

4-(3-Chloro-4-fluorophenylamino)-7-methoxy-6-[2-{4-(4-fluorophenyl)piperazin-1-yl}-2-oxo]-ethoxyquinazoline (**13**): Yield (0.11 g, 53.40%), m.p. 198–200 °C. FT-IR ν_{max} (KBr): 3357.77 (N–H), 2932.45 (asymmetric aliphatic C–H), 2832.48 (symmetric aliphatic C–H), 1645.08 (amide C=O), 1580.29 (C=N), 1505.93, 1430.81, 1282.60, 1220.57 (asymmetric C–O–C), 1145.62 (C–F), 1062.01 (C-Cl), 1024.38 (symmetric C–O–C), 817.83 cm^{-1}. ^{1}H NMR (DMSO-d_6): δ 3.11 (br s, 2H, -NCH_2-, piperazine), 3.20 (br s, 2H, -NCH_2-, piperazine), 3.74 (br s, 4H, -N(CH_2)$_2$-, piperazine), 3.97 (s, 3H, -OCH_3), 4.99 (s, 2H, -OCH_2-), 6.93-7.02 (m, 4H, Ar*H*, 4-fluorophenyl), 7.19 (s, 1H, Ar*H*, quinazoline), 7.25 (t, 1H, $J_o = 8.96$ Hz, Ar*H*, *ortho* to fluoro), 7.76–7.80 (m, 1H, Ar*H, ortho* to chloro), 7.83 (s, 1H, Ar*H*, quinazoline), 8.10 (dd, 1H, $J_o = 6.78$ Hz, $J_m = 2.58$ Hz, Ar*H*, *meta* to fluoro), 8.50 (s, 1H, -N = C*H*-N) and 9.42 ppm (s, 1H, -N*H*-). ^{13}C NMR (DMSO-d_6): δ 41.36 (N**C**H$_2$, piperazine), 44.60 (N**C**H$_2$, piperazine), 49.35 (N**C**H$_2$, piperazine), 49.70 (N**C**H$_2$, piperazine), 55.86 (O**C**H$_3$), 67.35 (O**C**H$_2$), 103.75 (Ar**C**H), 107.38 (Ar**C**H), 108.69 (Ar**C**), 115.26 (2 × Ar**C**H, $^2J_{C\text{-}F} = 22$ Hz), 116.27 (Ar**C**H, $^2J_{C\text{-}F} = 21$ Hz), 117.84 (2 × Ar**C**H, $^3J_{C\text{-}F} = 7$ Hz), 119.03 (Ar**C**, $^2J_{C(Cl)\text{-}F} = 18$ Hz), 121.87 (Ar**C**H, $^3J_{C\text{-}F} = 7$ Hz), 123.24 (Ar**C**H), 136.62 (Ar**C**), 147.29 (Ar**C**), 147.56 (Ar**C**), 147.58 (Ar**C**), 152.82 (N = **C**H-N), 153.25 (Ar**C**, $^1J_{C\text{-}F} = 249$ Hz), 155.27 (Ar**C**), 156.09 (Ar**C**), 157.63 (Ar**C**) and 165.13 ppm (**C**=O). ESI-MS m/z: 538.60 $[M\text{-}H]^+$, 540.26 $[M + H]^+$. Anal. calcd for $C_{27}H_{24}ClF_2N_5O_3$: C, 60.06; H, 4.48; N, 12.97 %. Found: C, 59.74; H, 4.22; N, 13.19%.

4-(3-Chloro-4-fluorophenylamino)-7-methoxy-6-[2-(pyrrolidin-1-yl)-2-oxo]ethoxyquinazoline (**14**) (0.11 g, 50.23%), m.p. 238–239 °C. FT-IR ν_{max} (KBr): 3340.15 (N–H), 2976.09 (asymmetric aliphatic C–H), 2887.27 (symmetric aliphatic C–H), 1637.95 (amide C=O), 1582.27 (C=N), 1504.66, 1432.38, 1286.74, 1224.26 (asymmetric C–O–C), 1148.59 (C–F), 1083.69 (C-Cl), 1057.80 (symmetric C–O–C), 845.90 cm^{-1}. ^{1}H NMR (DMSO-d_6): δ 1.80 (p, 2H, $J = 6.71$ Hz, -CH_2-, pyrrolidine), 1.93 (p, 2H, $J = 6.70$ Hz, -CH_2-, pyrrolidine), 3.37 (t, 2H, $J = 6.80$ Hz, -NCH_2- pyrrolidine), 3.55 (t, 2H, $J = 6.70$ Hz, -NCH_2- pyrrolidine), 3.95 (s, 3H, -OCH_3), 4.88 (s, 2H, -OCH_2-), 7.22 (s, 1H, Ar*H*, quinazoline), 7.45 (t, 1H, $J_o = 9.10$ Hz, Ar*H*, *ortho* to fluoro), 7.73–7.76 (m, 1H, Ar*H*, *ortho* to chloro), 7.77 (s, 1H, Ar*H*, quinazoline), 8.11 (dd, 1H, $J_o = 6.84$ Hz, $J_m = 2.60$ Hz, Ar*H*, *meta* to fluoro), 8.50 (s, 1H, -N = C*H*-N) and 9.51 ppm (s, 1H, -N*H*-). ^{13}C NMR (DMSO-d_6): δ 23.98 (**C**H$_2$, pyrrolidine), 26.17 (**C**H$_2$, pyrrolidine), 45.58 (N**C**H$_2$, pyrrolidine), 46.17 (N**C**H$_2$, pyrrolidine), 56.41 (O**C**H$_3$), 67.83 (O**C**H$_2$), 103.77 (Ar**C**H), 107.91 (Ar**C**H), 109.04 (Ar**C**), 117.04 (Ar**C**H, $^2J_{C\text{-}F} = 22$ Hz), 119.29 (Ar**C**, $^2J_{C(Cl)\text{-}F} = 18$ Hz), 122.93 (Ar**C**H, $^3J_{C\text{-}F} = 7$ Hz), 124.04 (Ar**C**H), 137.16 (Ar**C**, $^4J_{C\text{-}F} = 3$ Hz), 147.67 (Ar**C**), 148.08 (Ar**C**), 153.30 (N = **C**H-N), 153.76 (Ar**C**, $^1J_{C\text{-}F} = 256$ Hz), 154.89 (Ar**C**), 156.56 (Ar**C**) and 165.51 ppm (**C**=O). ESI-MS m/z: 429.40 $[M\text{-}H]^+$, 431.10 $[M + H]^+$, 453.20 $[M + Na]^+$. Anal. calcd for $C_{21}H_{20}ClFN_4O_3$: C, 58.54; H, 4.68; N, 13.00%. Found: C, 58.80; H, 4.32; N, 12.82%.

4-(3-Chloro-4-fluorophenylamino)-7-methoxy-6-[2-(4-phenylpiperazin-1-yl)-2-oxo]ethoxy-quinazoline (**15**): Yield (0.13 g, 65.32%), m.p. 225–227 °C. FT-IR ν_{max} (KBr): 3348.45 (N–H), 2927.12 (asymmetric aliphatic C–H), 2818.80 (symmetric aliphatic C–H), 1644.60 (amide C=O), 1579.02 (C=N), 1502.24, 1428.01, 1282.39, 1222.22 (asymmetric C–O–C), 1141.85 (C–F), 1057.88 (C-Cl), 1020.71 (symmetric C–O–C), 848.07 cm^{-1}. ^{1}H NMR ($CDCl_3$): δ 3.00 (t, 2H, $J = 5.04$ Hz, -NCH_2-, piperazine), 3.12 (t, 2H, $J = 4.86$ Hz, -NCH_2-, piperazine), 3.67 (t, 2H, $J = 5.04$ Hz, -NCH_2-, piperazine), 3.72 (t, 2H, $J = 4.90$ Hz, -NCH_2-, piperazine), 3.81 (s, 3H, -OCH_3), 4.91 (s, 2H, -OCH_2-), 6.79–6.86 (m, 3H, Ar*H*, phenylpiperazine), 6.99 (t, 1H, $J_o = 8.80$ Hz, *ortho* to fluoro), 7.01 (s, 1H, Ar*H*, quinazoline), 7.19 (t, 2H, $J_o = 7.48$ Hz, Ar*H*, phenylpiperazine), 7.46–7.50 (m, 1H, Ar*H*, *ortho* to chloro), 7.55 (s, 1H, Ar*H*, quinazoline), 7.67 (dd, 1H, $J_o = 6.60$ Hz, $J_m = 2.60$ Hz, Ar*H*, *meta* to fluoro), 8.35 (s, 1H, -N*H*-, D_2O exchangeable) and 8.49 ppm (s, 1H, -N = C*H*-N). ^{13}C NMR ($CDCl_3$): δ 45.49 (N**C**H$_2$, piperazine), 49.22 (N**C**H$_2$, piperazine), 49.87 (N**C**H$_2$, piperazine), 50.61 (N**C**H$_2$, piperazine), 56.06 (O**C**H$_3$), 68.13 (O**C**H$_2$), 103.92 (Ar**C**H), 108.04 (Ar**C**H), 108.93 (Ar**C**), 116.23 (Ar**C**H, $^2J_{C\text{-}F} = 22$ Hz), 116.74 (2 × Ar**C**H), 120.46 (Ar**C**, $^2J_{C(Cl)\text{-}F} = 18$ Hz), 120.92 (Ar**C**H), 121.83 (Ar**C**H, $^3J_{C\text{-}F} = 7$ Hz), 123.94 (Ar**C**H), 129.33 (2 × Ar**C**H), 135.70 (Ar**C**, $^4J_{C\text{-}F} = 3$ Hz), 146.92 (Ar**C**), 147.93 (Ar**C**), 150.58 (Ar**C**), 153.90 (N = **C**H-N), 154.46 (Ar**C**, $^1J_{C\text{-}F} = 245$ Hz), 154.63 (Ar**C**), 156.56 (Ar**C**) and 166.89 ppm (**C**=O). ESI-MS m/z: 520.50 $[M\text{-}H]^+$, 522.10 $[M + H]^+$. Anal. calcd for $C_{27}H_{25}ClFN_5O_3$: C, 62.13; H, 4.83; N, 13.42%. Found: C, 62.41; H, 4.52; N, 13.76%.

4-(3-Chloro-4-fluorophenylamino)-7-methoxy-6-[2-{4-(4-nitrophenyl)piperazin-1-yl}-2-oxo] ethoxyquinazoline (**16**): Yield (0.105 g, 41.82%), m.p. 240–242 °C. FT-IR ν_{max} (KBr): 3362.71 (N–H), 2922.86 (asymmetric aliphatic C–H), 2848.27 (symmetric aliphatic C–H), 1638.52 (amide C=O), 1595.22 (C=N), 1502.27, 1430.92, 1321.95, 1229.41 (asymmetric C–O–C), 1110.65 (C–F), 1069.40

(C-Cl), 1021.10 (symmetric C–O–C), 826.15 cm^{-1}. ^{1}H NMR ($CDCl_3$): δ 3.56 (br s, 2H, -NCH_2-, piperazine), 3.64 (br s, 2H, -OCH_2-, piperazine), 3.75 (br s, 2H, -NCH_2-, piperazine), 3.79 (br s, 2H, -NCH_2-, piperazine), 3.99 (s, 3H, -OCH_3), 5.01 (s, 2H, -OCH_2-), 6.99 (d, 2H, J_o = 9.40 Hz, Ar*H*, *meta* to nitro), 7.22 (s, 1H, Ar*H*, quinazoline), 7.28 (t, 1H, J_o = 8.96 Hz, Ar*H*, *ortho* to fluoro), 7.77–7.81 (m, 1H, Ar*H*, *ortho* to chloro), 7.86 (s, 1H, Ar*H*, quinazoline), 8.08 (d, 2H, J_o = 9.40 Hz, Ar*H*, *ortho* to nitro), 8.11 (dd, 1H, J_o = 6.82 Hz, J_m = 2.56 Hz, Ar*H*, *meta* to fluoro), 8.51 (s, 1H, -N = C*H*-N) and 9.45 ppm (s, 1H, -N*H*-). ^{13}C NMR (DMSO-d_6): δ 40.83 (N**C**H_2, piperazine), 43.71 (N**C**H_2, piperazine), 45.79 (N**C**H_2, piperazine), 46.13 (N**C**H_2, piperazine), 55.98 (O**C**H_3), 67.15 (O**C**H_2), 103.69 (Ar**C**H), 107.48 (Ar**C**H), 108.57 (Ar**C**), 112.59 (2 × Ar**C**H), 116.56 (Ar**C**H, $^2J_{C\text{-}F}$ = 21 Hz), 118.80 (Ar**C**, $^2J_{C(Cl)\text{-}F}$ = 18 Hz), 122.20 (Ar**C**H, $^3J_{C\text{-}F}$ = 6 Hz), 123.32 (Ar**C**H), 125.71 (2 × Ar**C**H), 136.72 (Ar**C**), 137.02 (Ar**C**), 147.28 (Ar**C**), 147.36 (Ar**C**), 151.91 (Ar**C**), 152.89 (N = **C**H-N), 154.34 (Ar**C**), 154.55 (Ar**C**), 156.08 (Ar**C**) and 165.47 ppm (**C**=O). ESI-MS m/z: 565.50 $[M\text{-}H]^+$, 567.10 $[M + H]^+$. Anal. Calcd for $C_{27}H_{24}ClFN_6O_5$: C, 57.20; H, 4.27; N, 14.82%. Found: C, 56.98; H, 4.58; N, 14.68%.

4-(3-Chloro-4-fluorophenylamino)-6-[2-{2-(3,4-dimethoxyphenyl)ethylamino-2-oxo}ethoxy]-7-methoxyquinazoline (**17**): Yield (0.17 g, 61.60%), m.p. 188–190 °C. FT-IR ν_{max} (KBr): 3344.11 (N–H stretch), 3081.75, 2934.26 (asymmetric aliphatic C–H), 2847.30 (symmetric aliphatic C–H), 1665.94 (amide C=O), 1631.29, 1580.78 (C=N), 1506.40, 1430.25, 1257.00, 1227.66 (asymmetric C–O–C), 1147.34 (C–F), 1068.50 (C-Cl), 1026.46 (symmetric C–O–C), 846.14 cm^{-1}. ^{1}H NMR (DMSO-d_6): δ 2.76 (t, 2H, J = 7.14 Hz, -NHCH_2CH_2-), 3.49 (q, 2H, J = 6.72 Hz, -NHCH_2-), 3.74 (s, 3H, -OCH_3), 3.75 (s, 3H, -OCH_3), 3.96 (s, 3H, -OCH_3), 4.67 (s, 2H, -OCH_2-), 6.71 (dd, 1H, J_o = 8.14 Hz, J_m = 1.86 Hz, Ar*H*, homoveratrylamine), 6.78 (d, 1H, J_o = 8.28 Hz, Ar*H*, homoveratrylamine), 6.79 (d, 1H, J_m = 1.48 Hz, Ar*H*, homoveratrylamine), 7.21 (s, 1H, Ar*H*, quinazoline), 7.30 (t, 1H, J_o = 8.98 Hz, Ar*H*, *ortho* to fluoro), 7.59 (t, 1H, J = 5.70 Hz, -CH_2N*H*-), 7.77–7.81 (m, 1H, Ar*H*, *ortho* to chloro), 7.88 (s, 1H, Ar*H*, quinazoline), 8.09 (dd, 1H, J_o = 6.80 Hz, J_m = 2.60 Hz, Ar*H*, *meta* to fluoro), 8.50 (s, 1H, -N = C*H*-N) and 9.45 ppm (s, 1H, -N*H*-). ^{13}C NMR (DMSO-d_6): δ 34.52 (NH**C**H_2**C**H_2), 55.17 (O**C**H_3), 55.31 (O**C**H_3), 55.62 (O**C**H_3), 68.07 (O**C**H_2), 103.88 (Ar**C**H), 107.30 (Ar**C**H), 108.58 (Ar**C**), 111.47 (Ar**C**H), 112.12 (Ar**C**H), 115.94 (Ar**C**H, $^2J_{C\text{-}F}$ = 22 Hz), 119.02 (Ar**C**), 120.29 (Ar**C**H), 121.68 (Ar**C**H, $^3J_{C\text{-}F}$ = 6 Hz), 123.22 (Ar**C**H), 131.25 (Ar**C**), 136.37 (Ar**C**), 146.76 (Ar**C**), 147.08 (Ar**C**), 147.32 (Ar**C**), 148.46 (Ar**C**), 152.80 (N = **C**H-N), 153.16 (Ar**C**, $^1J_{C\text{-}F}$ = 246 Hz), 154.09 (Ar**C**), 156.04 (Ar**C**) and 166.79 ppm (**C**=O). ESI-MS m/z: 541.17 $[M + H]^+$, 543.18 $[MH + 2]^+$, 563.14 $[M + Na]^+$. Anal. calcd for $C_{27}H_{26}ClFN_4O_5$: C, 59.95; H, 4.84; N, 10.36%. Found: C, 59.78; H, 4.99; N, 10.14%.

Biological activity

In vitro antiproliferative activity

The antiproliferative activity of the quinazoline analogues was carried out using NCI-60 screening protocol under Development Therapeutic Program of NCI as mentioned [18].

In vitro EGFR tyrosine kinase assay

The EGFR kinase assay kit (#40321) and Kinase-Glo® Max Luminescent kinase assay kit (#V6071) were obtained from BPS Bioscience (San Diego, CA) and Promega (Madison, WI), respectively. The positive control, erlotinib hydrochloride (#SML2156), and dimethyl sulfoxide (DMSO) were procured from Sigma-Aldrich (St Louis, MO).

To determine the inhibitory effects of the compounds **10-17** on wild type (WT) EGFR activity, the cell-free EGFR kinase Assay was carried out using the kit from BPS Bioscience (San Diego, CA). Erlotinib was used as the positive control. Erlotinib and test compounds were dissolved in DMSO to make a stock solution of 2.5 mM and 10 mM, respectively. They were subsequently diluted in distilled H_2O for the assay. WT EGFR, in a mixture with Kinase Buffer 1, ATP, and PTK substrate from the kit, was treated with test compounds of concentrations ranging from 1 nM to 10 μM in 10× dilutions; and 0.5, 1, 5, and 10 nM of erlotinib. The mixture was incubated at 30 °C for 40 min before the Kinase-Glo® Max reagent was added, and further incubation at room temperature was conducted for 3 h. Luminescence was then analysed with an integration time of 1000 ms using the Tecan (Switzerland) Spark 10 M plate reader.

Western blot study [19, 20]

MDA-MB-468 cells were grown in 6-well plates in media containing 10% (v/v) FBS till 90% confluence, after which they were exposed to 10 μM of each compound (**10** and **11**) for 1 h and afterwards treated with 100 ng/mL EGF (mpbio) for 15 min at 37 °C. Cells were then washed with cold PBS and then resuspended in 200 μL RIPA lysis buffer (SRL) containing protease and phosphatase inhibitor cocktail. After keeping the lysates on ice for 30 min they were centrifuged at 12,000 × *g* for 25 min at 4 °C. The supernatants were collected and Bradford assay was done to determine the protein concentration in the supernatant. SDS-PAGE loading buffer was used for the sample preparation and the sample solutions were then boiled for 10 min at 95 °C. Equal amounts of protein (10 μg) were loaded on SDS polyacrylamide gel (12%) electrophoresis and then transferred to a polyvinylidene difluoride membrane.

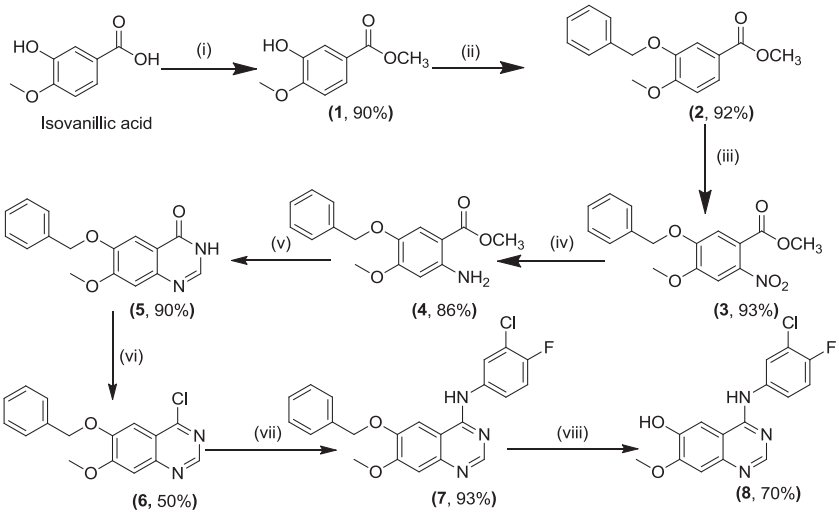

Scheme 1 Synthetic route for the preparation of 4-(3-chloro-4-fluoroanilino)-6-hydroxy-7-methoxyquinazoline (**8**). Reagents and conditions (i) MeOH, H_2SO_4, reflux; (ii) $C_6H_4CH_2Cl$, K_2CO_3, EMK, reflux; (iii) HNO_3, AcOH, 30 °C; (iv) Fe, NH_4Cl, MeOH and H_2O, reflux; (v) $HCONH_2$, AcOH, reflux; (vi) $POCl_3$, DMF (cat), reflux; (vii) 3-Cl,4-F-$C_6H_4NH_2$, *i*-PrOH, reflux; (viii) CF_3COOH, reflux, 1 h

Blocking buffer containing skimmed milk (5%) in TBS buffer was used to minimise nonspecific binding. Membranes were probed overnight with Phospho-EGF Receptor (1:2000, G-Biosciences) and β-actin (1:1000, CST) antibodies followed by incubation with horseradish peroxidase-conjugated (HRP) goat anti-rabbit IgG (1:3000, CST) for 1 h. Membranes were analysed using Amersham imager after incubation with enhanced chemiluminescence reagents (Bio-Rad).

Molecular docking

Schrödinger glide module was used to predict the binding interactions of the compound with the EGFR target protein. EGFR co-crystallised with lapatinib (PDB ID: 1XKK) with resolution 2.4 Å was downloaded from Protein Data Bank (www.rscb.org). Protein preparation wizard was used to process, optimise and minimise the protein with force field of OPLS 2005 and RMSD of 0.30 Å. Ligands were then drawn and imported in LigPrep wizard in which geometrically refined (cleaned) and the energy was minimised with force field OPLS-2005 and RMSD 1.0 Å. Prior to docking, receptor grid was generated by removing the co-crystallised ligand and position as well as size of the active site was determined. Glide XP docking program was used for the docking method. Per-residue interaction scores of each ligand were estimated in extra precision mode (Glide XP) using best 10 docking poses.

Results and discussion

Chemistry

The synthesis of key intermediate 4-(3-chloro-4-fluoroanilino)-6-hydroxy-7-methoxyquinazoline (**8**) was performed using the commercially available isovanillic acid as a starting compound as illustrated in Scheme 1. Isovanillic acid was esterified to methyl isovanillate (**1**) which upon treatment with benzyl chloride in the presence of potassium carbonate using ethyl methyl ketone as solvent yielded the benzyl protected methyl isovanillate **2**, nitration of which using glacial acetic acid and nitric acid afforded the nitro derivative **3**. Reduction of nitro group by iron and ammonium chloride in methanol yielded an amine **4**, which on further cyclization using formamide gave quinazoline **5**. Subsequent chlorination formed chloroquinazoline derivative **6**. Further reaction with 3-chloro-4-fluoroaniline afforded substituted 4-anilinoquinazoline **7**. Deprotection of compound **7** using trifluoroacetic acid yielded the desired intermediate 6-hydroxyquinazoline derivative **8** [21–24].

The target amide derivatives **10-17** were synthesised by esterification of compound **8** with methyl chloroacetate to yield quinazoline carboxylate **9** and its subsequent thermal fusion with various amines as depicted in Scheme 2. The structures of these analogues were determined by FT-IR, ^{1}H NMR, ^{13}C NMR and mass spectral analyses. The purity of all the quinazoline analogues was established by elemental analysis, which was within limits i.e., ±0.4 of calculated values.

Biological activity

In vitro antiproliferative assay

All the new quinazolines analogues **10-17** were selected by National Cancer Institute, Bethesda, USA for in vitro anticancer evaluation. The screening was done against a panel of 60 cell lines belonging to human leukaemia, non-small cell lung, colon, central nervous system, melanoma, ovarian, renal, breast and prostate cancer. Sulforhodamine B (SRB) assay was used for the screening of cellular proliferation. Growth percent of cells treated with quinazoline analogues **10-17** at 10 μM is shown in Table 1. All the compounds were found to display

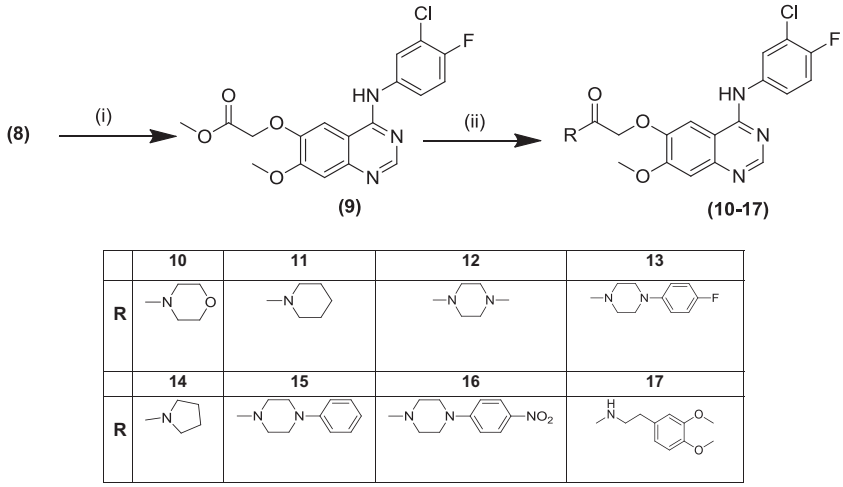

Scheme 2 Synthetic route for the preparation of gefitinib analogues **10-17**. Reagents and reaction conditions: (i) methyl chloroacetate, DMF, anhydrous K_2CO_3; (ii) requisite amine, fusion

potent and selective antiproliferative activity against several EGFR overexpressing solid tumour cell lines corresponding to non-small cell lung cancer, ovarian cancer, renal and breast cancer. In particular, the quinazoline derivatives **10-17** displayed prominent and selective inhibitory effects against NCI-H322M and NCI-H522 (~65%, non-small cell lung cancer), IGROV1 and SK-OV-3 (~50–80%, ovarian cancer), TK-10 (~50–80%, renal cancer) and MDA-MB-468 (~100%, breast cancer) tumour cell lines. The morpholine (**10**), piperidine (**11**) and *N*-methyl piperazine (**12**) derived analogues were found to be the most effective. They displayed inhibition of the order of 82.55%, 78.67% and 86.25%, respectively, against ovarian cancer SK-OV-3 cell lines and ~80% against renal cancer TK-10 cell line. The antiproliferative effects are comparable to standard drug gefitinib (NSC 759856) which produced 57.2%, 83% and 73% growth inhibition of IGROV1, SK-OV-3 and TK-10 cell lines, respectively, at 10 µM. The potency against the cell lines decreased on increasing the length of amine substituted side chain. The six membered heterocyclic amine remains the most favourable structural feature to be substituted on the side chain at 6- position of quinazoline ring for antiproliferative activity. The 4-aminoquinazoline derivatives **10-17** produced maximum activity against EGFR overexpressed MDA-MB-468 breast cancer cell line. The negative growth percentages (−41 to −7%) of this cell line after treatment with these compounds indicated not only decreased growth but also death of cancer cells. Piperidine substituted gefitinib analogue **11** produced maximum cytotoxicity (42%) against this cell line as compared to gefitinib (32%).

In vitro EGFR kinase inhibition assay

As the current series of quinazoline derivatives exhibited remarkable cytotoxicity against several solid tumour cell lines with high expression of wild type EGFR, therefore, the inhibitory effects of the compounds against EGFR tyrosine kinase were also determined. Initially evaluation of EGFR kinase inhibitory activity of new compounds was carried out at 10 µM using ELISA kits. All the synthesised analogues displayed more than 90% inhibition of EGFR at 10 µM except pyrrolidine substituted quinazoline **14** (75% inhibition) as shown in Table 2. The compounds **10**, **13**, **15–17** depicting maximum inhibition were further evaluated using a five-dose concentration panel to obtain the IC_{50} values (see supplementary information, Fig. S1). The morpholine substituted quinazoline **10** was found to be the highly potent inhibitor of EGFR ($IC_{50} = 6.12$ nM) amongst all with activity comparable to reference drug erlotinib ($IC_{50} = 1.37$ nM) and gefitinib ($IC_{50} = 3.22$ nM) [25]. Homoveratrylamine substituted quinazoline **17** also exhibited high EGFR inhibition with $IC_{50} = 8.78$ nM. These observations indicate that the antitumor effects of the compounds are very likely through inhibition of EGFR signalling pathway.

Inhibition of EGFR phosphorylation

Many of the research findings show that EGFR signal transduction is crucial for various vital cellular processes. To comprehend the mechanism of this series of compounds for antineoplastic activity, their role in the activation of EGFR in MDA-MB-468 cells was studied using western blot analysis. As morpholine substituted quinazoline analogue **10** was the most potent in vitro EGFR kinase inhibitor and piperidine derived compound **11** displayed maximum cytotoxicity against EGFR overexpressing MDA-MB-468 breast cancer cell line, these two compounds were selected for the analysis. It was observed that both the representative quinazoline analogues at 10 µM produced significant inhibition of phosphorylation of EGFR resulting in inactivation of the receptor and its downstream signalling proteins (Fig. 2, see supplementary information, Fig. S2 for full image). Quantitative analysis of western bolt revealed around 42% and 58% inhibition of phosphorylated EGFR in EGF induced MDA-MB-468 cells by the compounds **10**

Table 1 Growth percent of cells treated with quinazoline analogues **10-17** at 10 μM

Cancer cell line	10	11	12	13	14	15	16	17
Leukaemia								
CCRF-CEM	91.58	94.17	87.03	112.55	93.23	102.99	96.40	100.06
K-562	88.40	73.60	82.77	83.63	99.79	85.19	96.64	111.53
MOLT-4	91.55	73.84	81.16	85.84	105.01	90.27	94.12	93.42
RPMI-8226	90.99	81.92	90.55	98.75	96.84	83.65	94.05	90.13
SR	89.31	74.56	74.45	79.01	78.71	84.36	90.06	82.32
Non-small cell lung cancer								
A-549/ATCC	74.78	67.82	76.92	79.69	86.76	82.88	94.16	84.82
EKVX	63.31	63.55	61.77	78.31	89.18	77.64	85.05	78.19
HOP-62	98.09	102.75	96.94	95.23	103.96	102.78	98.91	95.65
HOP-92	92.05	81.65	75.14	87.89	88.27	86.83	88.75	87.90
NCI-H226	101.76	86.82	102.06	96.33	104.68	92.47	98.84	98.52
NCI-H23	90.69	90.96	98.11	97.00	88.31	88.00	96.02	92.54
NCI-H322M	**24.67**	**28.95**	**26.64**	**36.46**	**39.44**	**33.99**	54.23	**27.30**
NCI-H460	99.49	95.47	103.92	101.17	92.74	95.65	99.40	95.68
NCI-H522	**33.05**	**33.09**	**39.18**	72.17	86.58	79.95	76.12	70.23
Colon cancer								
COLO-205	105.69	96.03	104.21	101.23	115.82	111.79	101.64	101.72
HCC-2998	94.33	92.67	101.95	98.11	95.62	97.82	90.63	100.74
HCT-116	83.95	79.59	91.34	88.66	81.76	67.72	83.40	106.51
HCT-15	96.59	86.15	93.38	92.70	97.90	90.66	92.64	91.19
HT29	91.81	77.07	90.57	86.66	102.94	90.44	99.05	95.46
KM12	94.42	95.44	96.36	100.50	98.92	101.78	96.10	96.64
SW-620	102.13	104.00	104.86	100.91	94.59	101.23	98.02	100.50
CNS cancer								
SF-268	75.26	80.02	73.61	79.52	92.56	82.64	87.18	85.72
SF-295	90.63	92.07	92.79	94.13	92.64	93.35	103.89	98.05
SF-539	97.67	103.56	98.24	100.35	91.28	104.11	94.55	103.47
SNB-19	85.99	91.76	79.60	83.55	93.99	85.94	87.66	84.17
SNB-75	101.60	87.70	92.15	91.21	94.62	83.69	93.34	94.64
U251	101.86	96.85	101.45	107.07	97.19	98.87	106.07	102.52
Melanoma								
LOX IMVI	97.85	87.38	91.50	93.27	91.62	93.69	95.85	90.09
MALME-3M	98.22	99.09	96.51	92.20	92.23	96.34	88.74	86.93
M-14	90.41	85.51	97.45	81.26	93.85	99.40	96.53	101.27
MDA-MB-435	101.71	95.34	102.18	96.51	101.42	95.65	100.00	97.21
SK-MEL-2	87.12	88.13	94.43	97.54	103.85	101.54	107.26	86.95
SK-MEL-28	105.67	99.20	101.72	98.37	105.26	113.41	99.62	98.38
SK-MEL-5	98.40	90.36	97.52	98.20	104.86	95.04	100.63	92.49
UACC-257	106.14	101.41	104.42	113.87	108.47	106.92	102.31	110.28
UACC-62	86.63	91.68	98.10	87.90	93.05	92.80	91.27	95.74
Ovarian cancer								
IGROV1	**45.57**	**42.76**	**48.24**	**46.88**	**53.86**	**48.94**	**55.95**	**46.34**
OVCAR-3	79.69	73.16	78.15	83.44	89.07	87.77	88.41	82.84
OVCAR-4	82.66	71.65	79.47	81.98	95.04	85.65	95.96	92.36
OVCAR-5	74.05	67.01	78.39	60.49	78.84	75.04	84.80	65.39
OVCAR-8	87.20	89.19	89.96	106.77	97.45	93.50	96.90	102.79

Table 1 (continued)

Cancer cell line	10	11	12	13	14	15	16	17
NCI/ADR-RES	81.94	62.06	86.73	82.67	87.63	80.51	91.25	85.58
SK-OV-3	**17.45**	**21.33**	**13.75**	88.14	108.18	96.03	114.52	89.76
Renal cancer								
786-0	78.53	78.16	70.87	78.98	86.98	85.64	82.14	89.41
A-498	66.16	43.55	69.93	72.45	69.40	61.23	70.96	55.60
ACHN	31.89	32.17	37.78	45.93	54.77	50.57	55.93	49.00
CAKI-1	48.41	44.52	44.08	44.77	61.49	50.56	75.23	46.55
RXF-393	106.77	84.78	88.77	102.64	116.54	81.15	112.45	95.97
SN-12C	80.31	76.37	76.93	88.20	96.90	80.40	89.68	85.21
TK-10	**20.80**	**23.85**	**23.41**	**38.19**	**51.45**	**42.43**	**52.06**	**37.36**
UO-31	52.40	43.52	55.93	44.45	54.72	46.50	49.93	46.80
Prostate cancer								
PC-3	94.28	84.57	85.96	94.62	100.04	90.58	98.49	92.07
DU-145	57.28	53.83	62.60	60.50	78.26	62.86	79.29	57.96
Breast cancer								
MCF7	83.89	82.61	80.40	83.75	99.68	90.01	91.06	91.92
MDA-MB-231	107.97	105.36	94.70	79.28	94.06	90.48	89.73	94.39
HS 578 T	96.71	94.44	93.43	89.31	90.89	93.90	105.37	92.37
BT-549	98.53	94.42	89.61	100.68	96.76	106.18	92.65	99.45
T-47D	53.46	43.60	69.96	75.24	93.16	77.14	101.98	69.99
MDA-MB-468	**−15.88**	**−41.90**	**−32.42**	**−7.58**	**10.59**	**−17.47**	**33.93**	**−10.12**

Bold values represent high potency (growth inhibition/cytotoxicity) against specific cancer cell lines

Table 2 In vitro EGFR kinase inhibition after treatment with various compounds

Compound no.	% EGFR inhibition at 10 µM	IC_{50} (nM)
10	96.51	6.122
11	92.02	N.D
12	88.32	N.D
13	98.50	29.19
14	75.41	N.D
15	93.68	170
16	93.43	37.07
17	93.55	8.78
Erlotinib (positive control)	100	1.37

N.D not determined

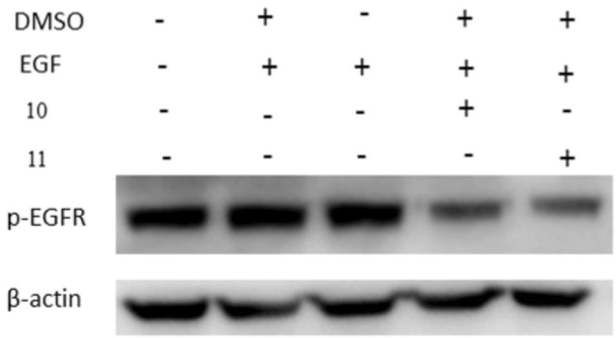

Fig. 2 Western blot analysis presenting the effects of quinazolines **10** and **11** on the phosphorylation of EGFR in MDA-MB-468 cells

and **11**, respectively (see supplementary information, Fig. S3). The results imply that these compounds exert their antiproliferative effects through the downregulation of EGF/EGFR signalling pathway.

Molecular docking

The binding interactions of the representative compound **10** were studied using Maestro 10.5 module, Schrodinger software by docking into the active ATP-binding site of EGFR. The crystal structure of EGFR/lapatinib complex (PDB ID: 1XKK) was used for the molecular docking analysis. N^1 of quinazoline scaffold of co-crystallised ligand lapatinib exhibited hydrogen bonding interactions with Met793 in the hinge region surrounded by Leu844, Gly796, Leu718 and Leu792 amino acid residues. The 2D and 3D diagrams depicting binding interactions of compound **10** have been presented in Fig. 3. The quinazoline core of compound **10** fitted well into the active ATP-binding site and display hydrogen bonding interaction with key amino

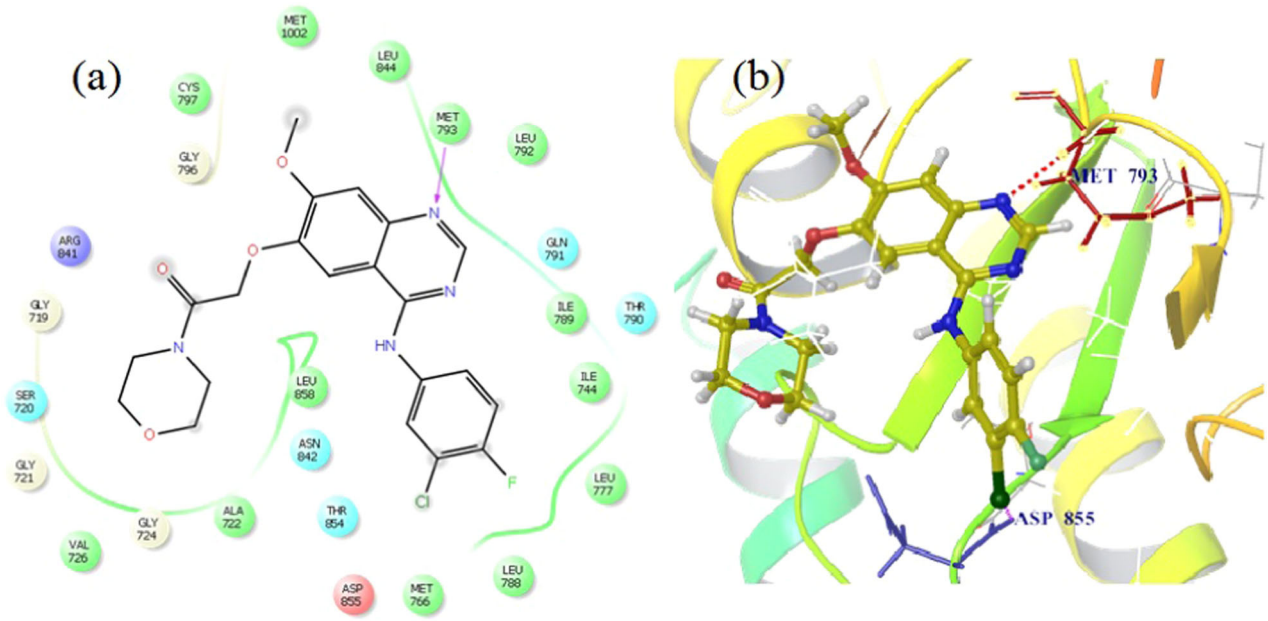

Fig. 3 Binding interactions of quinazoline **10** in the active site of crystal structure of EGFR (PDB ID 1XKK): (**a**) 2-D ligand binding interaction (**b**) 3-D ligand binding interaction; hydrogen bonding with the amino acid residues Met793 (red); polar interaction with Asp855 (purple dotted)

acid Met793 in a similar pattern as lapatinib and gefitinib [25, 26]. The extension of fluoro substituent towards the side chains of Met766 and interaction of chloro group with the highly conserved Asp855 residue account for the improved binding affinity.

Literature reports that substantial toxicity of second-generation irreversible inhibitors is due to covalent interaction of Michael group with Cys797 amino acid residue. As any such interaction with Cys797 was not observed in case of quinazoline **10** (Fig. 3), the analogue could be considered as a safe and reversible EGFR inhibitor. The positive interactions between EGFR and the new quinazoline analogue **10** further support the in vitro EGFR inhibitory activity data of this series of compounds.

Conclusion

Several 4,6,7-trisubstituted quinazoline derivatives have been prepared as potent EGFR inhibitors with improved and selective antiproliferative activity against several solid tumour cell lines. The analogue **10** substituted with a morpholine ring in the side chain at 6- position of quinazoline nucleus represents the most potent compound of the series with strong EGFR inhibition ($IC_{50} = 6.122$ nM) and ~80% growth inhibition against several solid tumour cell lines and lethality against MDA-MB-468 cells. Inhibition of phosphorylated EGFR in Western blot study using MDA-MB-468 cells further supported EGFR inhibition as a possible mechanism for antiproliferative activity of the quinazoline analogues. Quinazoline **10** when docked to the recognised binding sites of the EGFR fitted nicely and exhibited favourable interactions with key amino acid residue Met793, which account for its excellent inhibition of EGFR. It is illustrated that presence of a six membered heterocyclic amine on the side chain at 6- position of quinazoline ring remains the most favourable structural feature for antiproliferative activity as well as for the inhibition of EGFR. Increase in the length of amine substituted side chain at 6- position of the core nucleus results in comparatively low activity. The findings of this research work have led to the development of a lead molecule **10**, which could be further investigated to develop potent quinazoline based agents for the treatment of EGFR positive cancers.

Acknowledgements AM and RB are thankful to Department of Science & Technology, New Delhi for the financial support through INSPIRE fellowship (IF 140866). The authors express appreciation to National Cancer Institute, Bethesda, Maryland, USA for carrying out in vitro antineoplastic activity. CTY and APK are thankful to National Medical Research Council-CIRG, Singapore for financial support (R-185-000-353-213). APK was also supported by National Research Foundation, Singapore.

Compliance with ethical standards

Conflict of interest The authors declare that they have no conflict of interest.

Publisher's note Springer Nature remains neutral with regard to jurisdictional claims in published maps and institutional affiliations.

References

1. Ji Y, Sun Q, Zhang J, Hu H (2018) MiR-615 inhibits cell proliferation, migration and invasion by targeting EGFR in human glioblastoma. Biochem Biophys Res Commun 499:719–26
2. Yewale C, Baradia D, Vhora I, Patil SK, Misra A (2013) Epidermal growth factor receptor targeting in cancer: a review of trends and strategies. Biomaterials 34:8690–707
3. Herbst RS (2004) Review of epidermal growth factor receptor biology. Int J Radiat Oncol Biol Phys 59:21–26
4. Singh D, Attri BK, Gill RK, Bariwal J (2016) Review on EGFR inhibitors: critical updates. Mini-Rev Med Chem 16:1134–66
5. Killock D (2015) Lung cancer: a new generation of EGFR inhibition. Nat Rev Clin Oncol 12:373
6. Seshacharyulu P, Ponnusamy MP, Haridas D, Jain M, Ganti AK, Batra SK (2012) Targeting the EGFR signaling pathway in cancer therapy. Expert Opin Ther Targets 16:15–31
7. Housman G, Byler S, Heerboth S, Lapinska K, Longacre M, Snyder N et al. (2014) Drug resistance in cancer: an overview. Cancers 6:1769–92
8. Cockerill GS, Lackey KE (2002) Small molecule inhibitors of the class 1 receptor tyrosine kinase family. Curr Top Med Chem 2:1001–10
9. Kazandjian D, Blumenthal GM, Yuan W, He K, Keegan P, Pazdur R (2016) FDA approval of gefitinib for the treatment of patients with metastatic EGFR mutation-positive non-small cell lung cancer. Clin Cancer Res 22:1307–12
10. Barker AJ, Gibson KH, Grundy W, Godfrey AA, Barlow JJ, Healy MP et al. (2001) Studies leading to the identification of ZD1839 (IRESSA): an orally active, selective epidermal growth factor receptor tyrosine kinase inhibitor targeted to the treatment of cancer. Bioorg Med Chem Lett 11:1911–4
11. Dungo RT, Keating GM (2013) Afatinib first global approval. Drugs.Afatinib first global approval. Drugs 73:1503–15
12. Schwartz PA, Kuzmic P, Solowiej J, Bergqvist S, Bolanos B, Almaden C et al. (2014) Covalent EGFR inhibitor analysis reveals importance of reversible interactions to potency and mechanisms of drug resistance. Proc Natl Acad Sci USA 111:173–8
13. Xia GX, Chen WT, Zhang J, Shao JA, Zhang Y, Huang W et al. (2014) A chemical tuned strategy to develop novel irreversible EGFR-TK inhibitors with improved safety and pharmacokinetic profiles. J Med Chem 57:9889–9900
14. Li DD, Fang F, Li JR, Du QR, Sun J, Gong HB et al. (2012) Discovery of 6-substituted 4-anilinoquinazolines with dioxygenated rings as novel EGFR tyrosine kinase inhibitors. Bioorg Med Chem Lett 22:5870–5
15. Lü S, Zheng W, Ji L, Luo Q, Hao X, Li X et al. (2013) Synthesis, characterization, screening and docking analysis of 4-anilinoquinazoline derivatives as tyrosine kinase inhibitors. Eur J Med Chem 61:84–94
16. Das D, Hong J (2019) Recent advancements of 4-aminoquinazoline derivatives as kinase inhibitors and their applications in medicinal chemistry. Eur J Med Chem 170:55–72
17. Zhang L, Yang Y, Zhou H, Zheng Q, Li Y, Zheng S et al. (2015) Structure-activity study of quinazoline derivatives leading to the discovery of potent EGFR-T790M inhibitors. Eur J Med Chem 102:445–63
18. Shoemaker RH (2006) The NCI60 human tumor cell line anticancer drug screening. Nat Rev Cancer 6:813–23
19. Hou W, Ren Y, Zhang Z, Sun H, Ma Y, Yan B (2018) Novel quinazoline derivatives bearing various 6-benzamide moieties as highly selective and potent EGFR inhibitors. Bioorg Med Chem 26:1740–50
20. Egger D, Bienz K (1994) Protein (western) blotting. Mol Biotechnol 1:289–305
21. Abraham S, Bhagwat S, Campbell BT, Chao Q, Faraoni R, Holladay MW, Lai AG, Rowbottom MW, Setti E, Sprankle KG. (2009) Preparation of quinazoline derivatives as RAF kinase modulators for treating cancers, inflammation and immune diseases. PCT Int Appl WO 2009117080 A1.
22. Kumar N, Chowdhary A, Gudaparthi O, Patel NG, Soni SK, Sharma P (2014) A simple and highly efficient process for synthesis of gefitinib. Indian J Chem 53B:1269–74
23. Chunhua J, Ling X, Jiang C. (2006) Process of preparation of quinazoline derivatives as gefitinib intermediates. Faming Zhuanli Shenqing Gongkai Shuomingshu CN1850807 A.
24. Helal CJ, Kang Z, Hou X, Pandit J, Chappie TA, Humphrey JM et al. (2011) Use of structure-based design to discover a potent, selectivein vivo active phosphodiesterase 10A inhibitor lead series for the treatment of schizophrenia. J Med Chem 54:4536–47
25. Chen L, Zhang Y, Liu J, Wang W, Li X, Zhao L et al. (2017) Novel 4-arylaminoquinazoline derivatives with (E)-propen-1-yl moiety as potent EGFR inhibitors with enhanced antiproliferative activities against tumor cells. Eur J Med Chem 138:689–97
26. Zhang Y, Zhang Y, Liu J, Chen L, Zhao L, Li B et al. (2017) Synthesis and in vitro biological evaluation of novel quinazoline derivatives. Bioorg Med Chem Lett 27:1584–1587